Journal of the European Ceramic Society **11** (1993) 431–438

Intragranular Crack Deflection and Crystallographic Slip in Si_3N_4/SiC Nano-Composites

Tanguy Rouxel,* Fumihiro Wakai

Ceramic Evaluation Division, Government Industrial Research Institute, 1-1, Hirate-cho, Kita-ku, Nagoya, 462 Japan

Manuel E. Brito

National Institute for Research in Inorganic Materials, 1-1, Tsukuba, Ibaraki, 305 Japan

Atsushi Iwamoto & Kansei Izaki

Mitsubishi Gas Chemical Company, 22, Wadai, Tsukuba-shi, Ibaraki, Japan

(Received 25 June 1992; revised version received 7 September 1992; accepted 18 September 1992)

Abstract

Crack deflection is a potential mechanism for toughening essentially brittle materials. Deflection generally occurs along grain boundaries and is enhanced by particles with high aspect ratios. Si_3N_4/SiC ceramic/ceramic composites contain elongated β Si_3N_4 grains as a major phase and provide a good illustration for this mechanism. As a result, such materials demonstrate a relatively good fracture toughness. It is shown in this study, using transmission electron microscopy (TEM), that transgranular cracks, which develop at low temperatures and/or high deformation rates (present case), may also be deflected by intragranular SiC inclusions. Cracks use the 100 planes and propagate along the ⟨100⟩ directions of the silicon nitride hexagonal lattice. Further, after large plastic deformations at high temperature, slip defects are observed in silicon nitride grains, with many step-like deviations ('cross' slip), and the slip system is found to be [001] {100}.

Bakanntlich kann eine Zähigkeitssteigerung spröder Werkstoffe über den Mechanismus der Rißumleitung erfolgen. Der Riß wird hierbei im allgemeinen längs der Korngrenzen umgeleitet, wobei dieser Vorgang durch die Präsenz von Teilchen mit hohen Formfaktoren begünstigt wird. Keramik/Keramik-Verbunde aus Si_3N_4/SiC enthalten als Matrixphase längliche β-Si_3N_4-Körner und eignen sich sehr gut zur Veranschaulichung dieses Mechanismus, der bei diesen Werkstoffen zu verhältnismäßig guten Werten der Bruchzähigkeit führt. In dieser Arbeit wird mittels Transmissionselektronenmikroskopie gezeigt, daß auch transgranulare Risse, die sich bei geringen Temperaturen und/oder bei hohen Verformungsgeschwindigkeiten gebildet haben (vorliegender Fall), durch intragranulare SiC-Einschlüsse abgeleitet werden können. Die Risse verlaufen längs {100}-Ebenen und breiten sich in den ⟨100⟩-Richtungen des hexagonalen Siliziumnitrid-Gitters aus. Nach großen plastischen Verformungen bei hohen Temperaturen können außerdem Gleitdefekte innerhalb der Siliziumnitrid-Körner auftreten, wobei zahlreiche stufenartige Defekte ('Quergleiten') beobachtet werden. Als Gleitsystem wurde [001] {100} festgestellt.

Il est clairement établi que le mécanisme de déviation de fissure peut permettre de renforcer des matériaux essentiellement fragiles. La fissure est généralement déviée le long des joints des grains et le phénomène est accentué par la présence de particules idiomorphes. Les composites céramiques Si_3N_4/SiC contiennent principalement des grains allongés β Si_3N_4 et fournissent une bonne illustration de ce mécanisme. De ce fait, ces matériaux ont une relativement bonne ténacité en comparaison des céramiques monolithiques SiC ou Si_3N_4. Nous montrons dans cette étude, à partir d'images de microscopie électronique en transmission, que des microfissures transgranulaires, qui sont susceptibles de se développer à basse température et/ou pour des vitesses de déformation élevées (cas présent), peuvent aussi être déviées, par

* Present address: Laboratoire de Matériaux Céramiques et Traitements de Surface, ENSCI, URA 320, 47 av. A Thomas, 87065 Limoges cédex, France.

Journal of the European Ceramic Society 0955-2219/93/$6.00

des particules SiC intragranulaires et nanométriques. Les fissures présentes dans de nombreux grains se propagent invariablement dans des plans {100} et suivant des directions ⟨100⟩ du réseau héxagonal du nitrure de silicium. Par ailleurs, pour des déformations plastiques importantes (>100%), à l'issue d'essais mécaniques à haute température (>1500°C), des défauts de glissement sont observés dans les grains de nitrure de silicium, sous la forme de marches à la surface des plans de base (001) (glissement dévié), et le système de glissement [001] {100} a été identifié.

1 Introduction

Taking advantage of the properties of both silicon nitride and silicon carbide covalently bonded crystals, Si_3N_4/SiC nano-composites are ceramic materials containing β Si_3N_4 grains (matrix) and SiC particles which are disseminated at grain boundaries as well as in the elongated Si_3N_4 grains. The denomination 'nano-composite' is justified by the nanometre size of the particles that are included in the silicon nitride grains.[1] Such a microstructure leads to exceptional thermo-mechanical properties.[2,3] For instance, due to both a very small grain size and an homogeneous microstructure, this highly covalent material exhibits a superplastic behaviour at elevated temperature,[4] provided that suitable sintering additives are added (Al_2O_3, Y_2O_3). Fracture toughness is found to be significantly improved as the volume fraction of silicon carbide increases from 0% (K1c = 5 MPa $m^{0.5}$) to 10% (K1c = 7 MPa $m^{0.5}$) but decreases for higher SiC volume fractions. The reinforcement was attributed to the increase of the silicon nitride grain aspect ratio (GAR = length/diameter) as the SiC content rises up to 10% with subsequent crack deflection and/or branching resulting from the acicular particles.[3] Above 10% SiC, the silicon nitride grain aspect ratio was found to decrease, resulting in a weakening of the material. Some TEM (transmission electron microscopy) investigations have already been conducted on similar materials. Niihara and colleagues[5] reported a very good interfacial lattice fitting between the intragranular SiC inclusions and Si_3N_4 with a limited atomic misfit and no interfacial phase. Sasaki and colleagues[6] found evidence for crack deflection in composites with less than 15 vol.% SiC and proposed the {100} and {101} crystallographic planes as easy cleavage planes in β Si_3N_4 grains. Earlier works on dislocation activity in β Si_3N_4 led Butler[7] to propose [001] and {100} as slip direction and plane respectively for the dislocation glide. More general microstructural observations dealing with cracks and defects in silicon nitride based materials showed the presence of planar defects in the {001} planes of α Si_3N_4, one of these being characterized by displacements in ⟨120⟩ directions.[8,9,10]

A question which arises with the ultrafine structure of nano-composite materials concerns the influence of elastic moduli and thermal expansion coefficient mismatch between the two coexisting crystalline phases on the thermal and mechanical behaviour of the composite. In particular, it is obvious that second phase particles provide heterogeneous regions with local strain/stress fields which are likely to alter the mechanical response of the material.

In this paper, we comment on some TEM pictures showing intragranular crack deflections. Two cases are examined: (i) crack initiation and arrest from a SiC particle and (ii) crystallographic slip in a Si_3N_4 grain with step-like deviations by SiC inclusions. Observations were almost limited to basal planes of silicon nitride crystals. The importance and the role of internal stresses on the crack-particle interactions and on the fracture behaviour will be discussed.

2 Materials

Material preparation has already been detailed elsewhere.[2] In this study, the ceramic material was sintered at 1700°C for one hour with 6 and 2 wt% yttria and alumina respectively as sintering aids. The SiC content is close to 30 vol.%. The matrix is composed of needle-like β Si_3N_4 grains, with average length and diameter of 1 and 0·3 μm respectively. Crystals have an hexagonal structure (space group $P6_3/m$), with a = 7·603 Å and c = 2·907 Å. Yttrium and aluminium are exclusively retained in the amorphous intergranular phase. SiC particles are disseminated either at grain boundaries, or in grains with a nanometre size in the latter case. For comparison with other materials, the following characteristic properties were measured at room temperature: density $\rho = 3{\cdot}3$ g/cm^3, hardness (Vickers test) H = 18·5 GPa, fracture toughness (SENB) K1c = 5·5 MPa $m^{0.5}$, fracture strength (4 points) $\sigma_r = 977$ MPa.

3 Observations

TEM preparation required mechanical polishing of plates of less than 0·2 mm up to 30 μm, using diamond disks and a dimpler equipment, and subsequent argon ion beam thinning. Low magnification and high resolution observations were conducted on JEOL 4000 FX and 2000 EX transmission electron microscopes operated at 400 and 200 kV respectively.

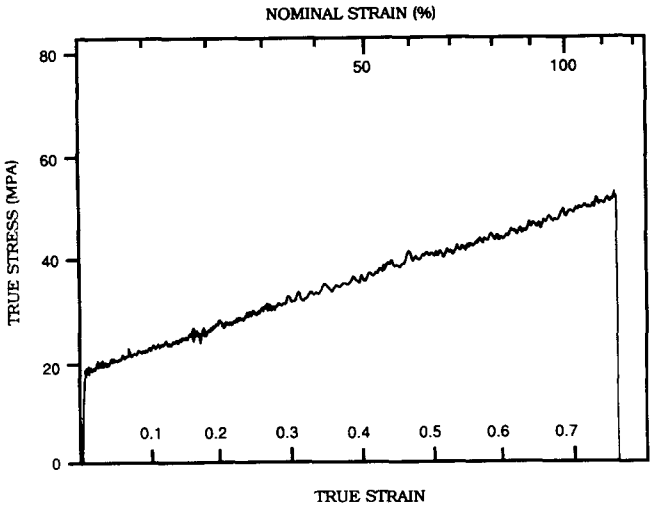

Fig. 1. Tensile test conducted under nitrogen atmosphere at 1600°C with a strain rate of 2×10^{-5}/sec.

Observed samples were cut from tensile specimens, perpendicularly to the tensile axis, after the ceramic was plastically deformed up to 114% elongation at 1600°C. The deformation curve is shown in Fig. 1. The elongation (also nominal strain) is given by:

$$\Delta l/l_0 = \exp(\varepsilon) - 1$$

where the true strain ε at time t is expressed by the Hencky relation:

$$\varepsilon = \ln(l/l_0)$$

where l_0 is the initial gauge length and l is the gauge length at time t. It has been shown[11] that such a large plastic deformation results in grain alignment toward the tensile axis, so that a cross-section shows nearly perfect hexagonal patterns, which are actually the basal planes of the β Si_3N_4 grains. Since no crack was observed in the as-sintered specimens, it is assumed that the observations we will further discuss are directly related to the high temperature deformation of the material.

Figure 2 shows a SiC inclusion trapped in a grain, with the c-axis almost parallel with the electron beam (see diffraction pattern), from which two straight cracks have propagated in planes containing the [100] and [010] directions of the matrix crystal. A similar event occurred, on a minor scale, in the grain labelled α. Both crack arrests are located inside the grain and high magnification of the crack tips reveals the surrounding strain field, effective upon a domain of about 30 nm radius around the tips. The tips seem to be almost atomically sharp. The image of the whole grain suggests that crack arrests are not due to natural lattice trapping but result from external stresses, applied by the surrounding grains. According to our observations, cracks propagate along $\langle 100 \rangle$ directions and there seems little doubt that crack walls are parallel to $\{100\}$

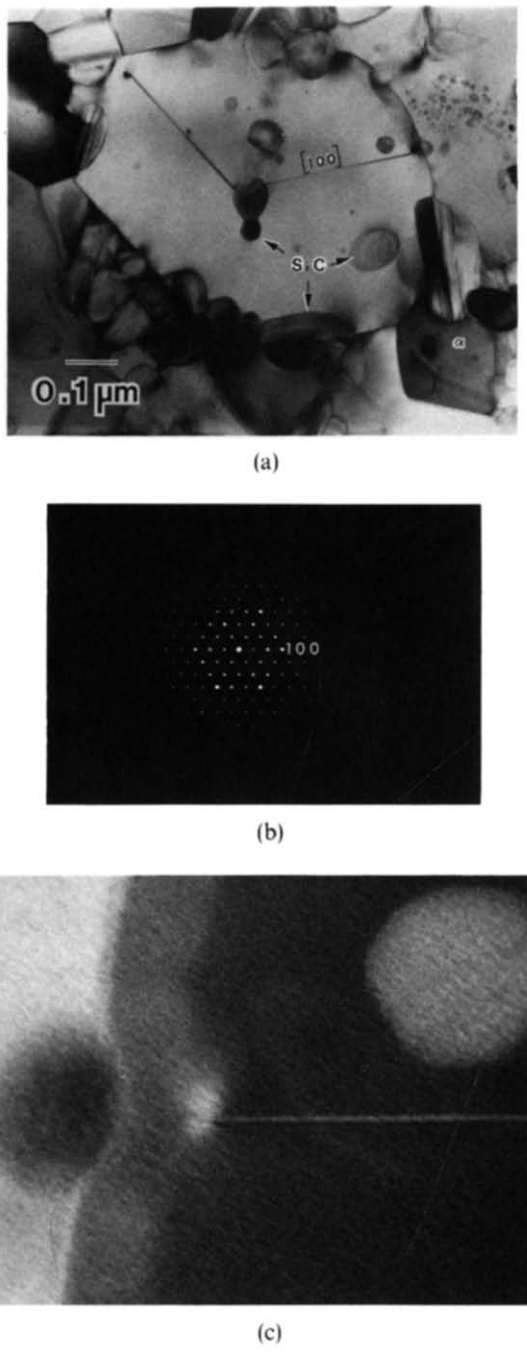

Fig. 2. (a) Image of an intragranular crack deflection in a basal plane of a βSi_3N_4 crystal. (b) Diffraction pattern on the silicon nitride grain. (c) Higher magnification view of a crack tip.

planes. Such planes are the most widely spaced of the crystal and contain the shortest lattice vector in the c-direction. The facet structure of the intragranular SiC particles (see for example the particle near the crack in Fig. 2c), in which facets coincide with $\{100\}$ planes of the silicon crystal, has already led Niihara and coworkers[5] to suggest that $\{100\}$ planes form low energy surfaces.[6] Thus, our observations are very consistent with earlier studies.[7,12] Since there is no opening displacement, the defect observed in Fig. 3 appears as an edge, which might arise from a slip process with a displacement component perpendicular to the figure, several times deflected by intragranular SiC inclusions, and dividing the basal

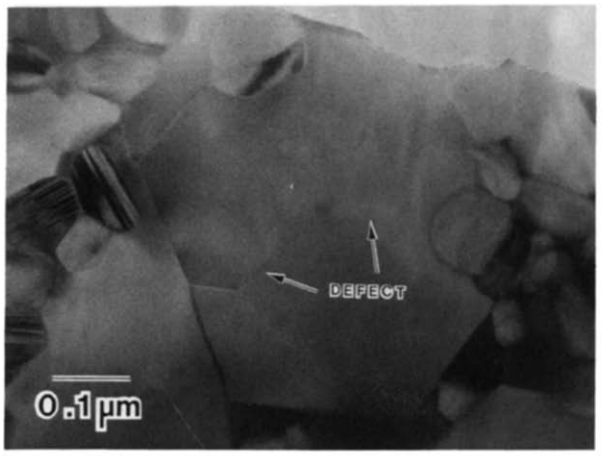

(a)

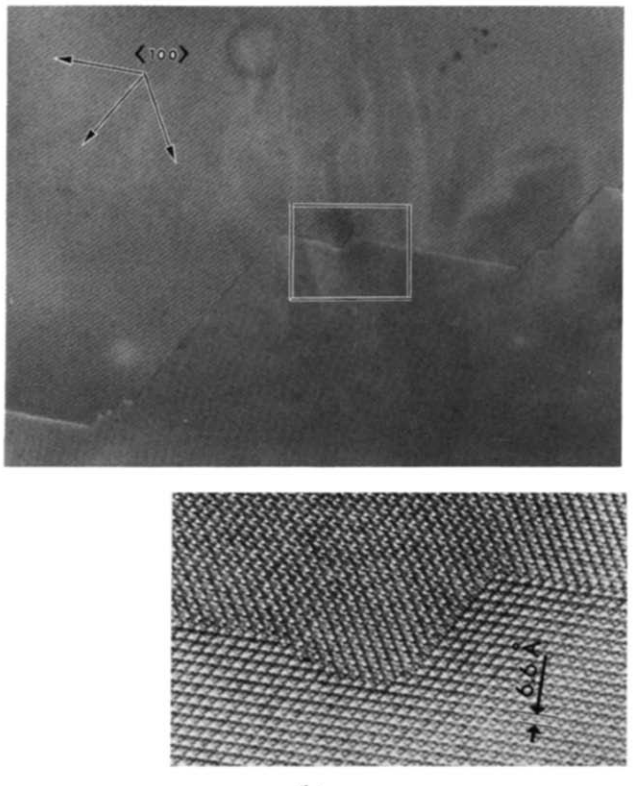

(b)

Fig. 3. (a) Image showing a transgranular defect with step-like deflections. (b) HREM image of the defect. The insert shows some details at higher magnification.

plane into two parts. The HREM image of the edge deflection around a particle clearly shows that the trajectory is formed by straight segments, all of them following ⟨100⟩ directions. Although only one inclusion appears to deviate from the edge in the figure, particles located in other basal planes, within the same Si_3N_4 crystal may have had similar effects. Thus, random distribution of SiC particles in the volume of the grain results in the numerous deflections ('cross' slip). It is remarkable that in both the studied cases, deflection occurs using ⟨100⟩ directions, with a tilt angle between two adjacent segments of the trajectory of $n \times 2\pi/3$ rad (n being an integer). Some observations in planes containing the tensile axis, like that of Fig. 4, reveal defects

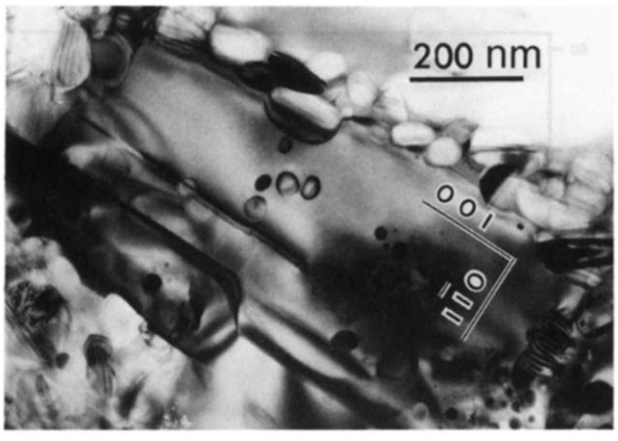

Fig. 4. View of silicon nitride grain along the tensile direction (e^- beam perpendicular to the c-axis of the grain).

(presumably from dislocation activity) along the [001] direction of βSi_3N_4 grains. There is therefore little doubt that prism slip occurred and the easy slip planes appear to coincide with the easy cleavage planes. Though it is not a sufficient criterion to determine the slip planes, it is interesting to note that for hexagonal crystals low c/a values tend to favour prism slip. Prism slip is observed in hard metals (hafnium, titanium, etc.) for which the c/a ratios (1·581 for Hf and 1·587 for Ti) are lower than that of an ideal hcp structure ($c/a = 1{\cdot}630$).[13] Prism slip was also observed in WC crystals ($c/a = 0{\cdot}976$).[14] When c/a becomes very small, like for βSi_3N_4 ($c/a = 0{\cdot}382$), the shortest slip vector is by far the [001] and the slip system is found to be [001] {100}.

It must be emphasized that the events recorded on the selected pictures were observed in many grains and are therefore a general feature of the deformed microstructure. Cracks were always localized to single grains and reflect a global damage of the bulk.

4 Discussion

We will attempt in this part to propose an explanation for the phenomenon of intragranular crack deflection and deviation around particles as well as for the cross-slip mechanism illustrated in Fig. 3. The energy required for cleavage (fracture) or for slip (plastic deformation) will be discussed with regard to the thermally originated elastic stress/strain fields which developed at particle sites after cooling from the sintering temperature. The analysis is based on the assumption that the crack path is the one that minimizes the work necessary to produce cleavage. It is therefore implicitly considered that the intragranular SiC particle dispersion does not provide any improvement of the fracture toughness, but indeed favours intragranular decohesion in silicon nitride crystals. The present approach is therefore quite different from the deflection tough-

ening analysis developed by Faber *et al.*[15] in the case of crack-particle interactions producing non-planar cracks subjected to lower stress intensity factors than those experienced by the corresponding planar cracks. In the following analysis, we consider a grain experiencing a shear stress parallel to the prism axis, so that cleavage in prismatic planes is favoured, allowing the stress intensity factor to be uniform along the crack front (with or without deflections). The crack surface is assumed to be limited to {100} planes, consistent with our observations, so that crack bowing or twisting around particles are not considered. A detailed analysis of particulate composites by Krstic *et al.*,[16] has already shown that no significant toughness improvement can be achieved, though a satisfactory bonding exists between the matrix and the second phase, as long as the Young's modulus and the thermal expansion coefficient of the particle are larger than those of the matrix. To go further on interpretation and to describe the mechanisms in terms of analytical expressions, basic arguments of continuum mechanics were used, assuming that both the matrix and the particle phases are linear elastic isotropic materials. This approach allows a first approximation evaluation of the stress and strain components. However, in order to obtain the exact solution, it would be necessary to introduce the five independent compliances of the βSi_3N_4 crystal and the compliances corresponding to the complex layered structure of SiC particles. Further, inclusions are taken as identical spheres of radius R, although the particle shape is not purely spherical but tends to be hexagonal, as previously reported,[5] and the periodic atomic misfit at the SiC/Si_3N_4 interface, which results in an angular dependence of the stress/strain fields, has been neglected.

4.1 Crack deflection mechanism

Let us first analyze the stress/strain fields in the vicinity of the intragranular SiC particles, using a continuum picture of the solids. It has been shown[17] that, in the absence of any long-range stress field, Young's modulus and thermal expansion coefficient mismatch lead to a stress tensor having three non-vanishing components; namely spherical coordinates σ_{rr}, $\sigma_{\theta\theta}$ and $\sigma_{\phi\phi}$, with, for the matrix surrounding the inclusion,

$$\varepsilon_{rr} = -2\varepsilon_{\theta\theta} = -2\varepsilon_{\phi\phi} = -(1+\nu_m)PR^3/(E_m r^3) \quad (1)$$

$$\sigma_{rr} = -2\sigma_{\theta\theta} = -2\sigma_{\phi\phi} = -PR^3/r^3 \quad (2)$$

and inside the particle:

$$\varepsilon_{rr} = \varepsilon_{\theta\theta} = \varepsilon_{\phi\phi} = -(1-2\nu_p)P/E_p \quad (3)$$

$$\sigma_{rr} = \sigma_{\theta\theta} = \sigma_{\phi\phi} = -P \quad (4)$$

with:

$$P = (\alpha_m - \alpha_p)\Delta T/[(1+\nu_m)/(2E_m) + (1-2\nu_p)/E_p] \quad (5)$$

where r is the distance to the centre of the particle ($r \geq R$), α is the thermal expansion coefficient, ΔT is the temperature deviation from the equilibrium state (no residual stress), ν is the Poisson ratio and E is the Young's modulus; subscripts m and p refer to the matrix and to the particle respectively. In the present case, α_p is assumed to be larger than α_m, as the temperature is below 1000°C (this will be further discussed) and, considering that residual stresses originate from the difference between the sintering temperature and the testing one, it appears that, outside the inclusion, the radial component (σ_{rr}) is a tensile stress whereas both the tangential normal components ($\sigma_{\theta\theta}$) and ($\sigma_{\phi\phi}$) are compressive stresses. Consequently, under critical conditions of crack appearance, the above expression predicts that a crack will develop tangentially with respect to the particle and that a propagating crack will be deflected around the SiC particles, consistent with our observations. This crack-particle interaction will result in a crack avoiding the particle completely. Further, if an external stress is superimposed, a crack approaching a spherical particle equatorially will experience a decrease of the stress intensity factor since the compressive tangential stress will tend to balance the applied far-field tensile stress. This may cause the deceleration of the crack velocity and results in a crack-trapping phenomenon as in Fig. 2. For a pure elastic fracture behaviour, otherwise neglecting the inertia forces, the appropriate statement of the global conservation of energy is expressed by:

$$W_f = 2\gamma S$$

where W_f is the work of fracture, S is the crack surface area (there are two walls) and γ is the intrinsic surface energy of the crack-generated free surface. The elastic distortions of the atomic network in the matrix near SiC particles after the value of γ and the former equation should be detailed to account for the various strain states of the matrix atomic network:

$$W_f = 2(n_p\gamma_p S_p + \gamma_m S_m + \gamma_r S_r) \quad (6)$$

where S_p, S_m and S_r are the crack surface areas around the particle in the matrix (far from the particle surface) and in the regions corresponding to the radial approach near the inclusion, respectively; n_p represents the number of particles intersecting with the crack surface. Around particles, $\varepsilon_{rr} > 0$ and the radial interatomic distance is higher than in the stress-free region, whereas $\varepsilon_{\theta\theta} < 0$ and the tangential interatomic distance is reduced, compared to its value at rest. Thus, it is intuitive that $\gamma_p < \gamma_m < \gamma_r$.

Nevertheless, since $|\varepsilon_{\theta\theta}|$ decreases rapidly as r increases ($1/r^3$), S_r will be neglected compared to S_p and S_m and eqn (6) becomes:

$$W_f = 2(n_p\gamma_p S_p + \gamma_m S_m) \quad (7)$$

Since the crack front is found to follow {100} crystallographic planes only, notwithstanding the numerous possible deflections, γ_m is homogeneous along the crack surface far from the particles. As crack advance proceeds around the SiC particles, interatomic debonding occurs and part of the elastic energy (W_e) stored in the particle is relaxed through its contribution to the crack length increment. W_e is expressed by:

$$W_e = 1/2 \int\int\int_{\vartheta_p} (\sigma:\varepsilon)\,dv \quad (8)$$

where ϑ_p is the volume of an inclusion and $\sigma:\varepsilon$ is the local elastic energy potential. It can be easily shown from eqns (3) and (4) that:

$$W_e = 2\pi P^2(1-2\nu_p)R^3/E_p \quad (9)$$

S_p being the surface area where debonding occurs, the contribution of the relaxed elastic energy to crack propagation may be estimated as follows:

$$\Delta W_e = kS_pW_e/(4\pi R^2)$$

where k is a calibration factor ($0{\cdot}5 < k < 1$) accounting for the stress redistribution following the breakage of interatomic bonds.

Therefore,

$$\gamma_p S_p = \gamma_m S_p - kS_pW_e/(4\pi R^2)$$

and

$$\gamma_p = \gamma_m - kW_e/(4\pi R^2) \quad (10)$$

Replacing the above expression in eqn (7), remembering that $S = S_m + n_pS_p$, gives:

$$W_f = 2[\gamma_m S - kn_pS_pW_e/(4\pi R^2)] \quad (11)$$

If f_p is the intragranular volume fraction of particles, and considering that the second phase exhibits spatial randomness throughout the matrix, simple probabilistics can be used to express n_p in terms of f_p, R and the whole crack surface area S. It is first remarked that f_p is also the surface fraction of particles in any planar section and, R_m being the average apparent radius of the particles in the section, this gives:

$$n_p = f_pS/(\pi R_m^2)$$

R_m corresponds to the usual expression, commonly used in fractographic analysis,

$$R_m = R\pi/4$$

and thus

$$n_p = 16f_pS/(\pi^3R^2) \quad (12)$$

From the expression for R_m, a value for the average debonded surface area can be estimated:

$$S_p = \pi^4R^2[\pi - (\pi^2-4)^{0{\cdot}5}]/32 \quad (13)$$

Combining eqns (11), (12), (13) and (9) finally gives:

$$W_f = 2\{\gamma_m - kf_p\pi^3P^2(1-2\nu_p) R[\pi-(\pi^2-4)^{0{\cdot}5}]/(32E_p)\}S \quad (14)$$

Deflection mechanisms involve an increase of the relevant surface area S. Therefore, it is energetically stable as long as $dW_f/dS \leq 0$, which according to eqn (14) leads to:

$$\gamma_m \leq kf_p\pi^3P^2(1-2\nu_p)R[\pi-(\pi^2-4)^{0{\cdot}5}]/(32E_p)$$

or

$$\gamma_m \leq 0{\cdot}7kf_pP^2R(1-2\nu_p)/E_p \quad (15)$$

The above inequality predicts that deflection is enhanced by high values of P, i.e. high temperature difference from the equilibrium state, by large particle size and by a high volume fraction of second phase. Further, it shows that cracks are more likely to propagate from one particle to another as the SiC volume fraction increases, providing an explanation to the decrease of the fracture toughness for high SiC content.

It must be remarked that, in practice, grains are not uniformly stressed and one must invoke the complex dynamic stress distribution which develops in each grain during deformation. In the elastic domain (during loading), grains are randomly orientated and there is only one stress component (pure tension) at both the microscopic and the macroscopic scales. As soon as the yield stress is reached, grain boundary sliding occurs and the initial uniform and elastic stress state is destroyed. Homogeneous viscous sliding is impeded by the presence of asperities on the surface of contiguous grains and by second phase particles located between the silicon nitride grains, which may result in local stresses at the contacting zones (see Fig. 2c) and cause the deviation of intragranular cracks.

4.2 Cross slip mechanism

Specimens that are studied here were mechanically tested at an exceptionally high temperature (above half the absolute melting temperature). Therefore, the possibility of crystallographic slip (as in Fig. 3) through dislocation activity must be examined. A detailed description of dislocation activity and dislocation/particle interaction is far beyond the scope of this paper. Discussion will be limited to some general aspects of slip in covalent crystals together with the influence of second phase particles on the slip characteristics.

In covalently bonded crystals, the amplitude of the critical shear stress τ_p required to overcome the

Peierls energy barrier is very high and strongly depends on the distance h between the slip planes as follows:

$$\tau_p = 2G_m/(1 - \nu_m)\exp[-2\pi h/(b(1 - \nu_m))] \quad (16)$$

where G_m is the shear modulus of the matrix and b is the amplitude of the slip vector (Burgers vector). Around SiC inclusions, the h/b ratio exhibits a strong increase so that, on one hand, τ_p is greatly reduced. On the other hand, the possibility of strengthening due to Orowan by-passing of the particles by the dislocations must also be considered. Due to dislocation accumulation at particles (dislocation loops), local stresses rise, and eventually local failure occurs. The cross-slip mechanism is therefore controlled by the competition between the various energetic terms governing the movement of a dislocation: energy increase due to (i) bowing of the dislocation line around particles and (ii) to an increase of the slip surface area as deviations occur, and energy reduction due to an increase of the h/b ratio around second phase particles. Although a precise analytical development has not been achieved here, the above mentioned arguments suggest that the cross-slip and the crack deflection mechanisms have many characteristics in common.

4.3 Comment on a quantitative evaluation

A major impediment to a quantitative evaluation of the strain and stress magnitude in and around the SiC particles, or to check the validity of inequality (15), lies in the lack of experimental data on the physical properties of the material above 1400 °C. At room temperature, using the commonly used data of the literature for a rough estimation,[18] $\alpha_m = 3{\cdot}4 \times 10^{-6}$/°C, $\alpha_p = 4{\cdot}5 \times 10^{-6}$/°C, $E_m = 310$ GPa, $E_p = 430$ GPa, $\nu_m = 0{\cdot}27$, $\nu_p = 0{\cdot}17$, $\gamma_m = 45$ J/m^2 (calculated from $\gamma = K1c^2(1 - \nu^2)/2E$), $R = 0{\cdot}1$ μm and further taking $k = 1$ and $\Delta T = 1700$ °C gives $P = -522$ MPa, $W_e = 2{\cdot}6 \times 10^{-15}$ J (enough to fracture an area of about 5·4 nm^2) and $dW_f/dS = 2(\gamma_m - 3 \times 10^{-3})$. In eqn (14), γ_m is much greater than the second term so that $W_f \approx 2\gamma_m S$. Thus, at relatively low temperature, the above calculation predicts that the energy available from the strain fields at particles sites will hardly affect the work of fracture, nor the crack propagation, except on the fine details of the crack path very near to a particle meeting the crack front. In fact, cracks are expected to propagate straight through the grain, as has been widely documented in previous fracture analysis at low temperature. However, at elevated temperatures (i.e. above 1200 °C), both the fracture toughness and the elastic moduli[19] decrease drastically so that both terms in inequality (15) are strongly altered compared to their values at room temperature. The studied composite was mechanically tested at such an elevated temperature that it could be plastically deformed, though it is a strongly covalently bonded material. To go further on interpretation, it would be required to measure the physical properties of the composite at such elevated temperatures.

5 Conclusion

Transmission electron microscope analysis of the microstructure of a Si_3N_4/SiC nano-composite after deformation at high temperature provides evidence for intragranular crack deflection. Cracks appeared to be deflected by nanometre-sized SiC inclusions along ⟨100⟩ directions. The {100} planes of the silicon nitride hexagonal lattice were found to be easy cleavage planes. A criterion for crack deflection has been proposed. The model developed applies in the case of hard particles (non-penetrable) embodied in a less hard matrix with thermo-elastic stresses driving a propagating crack around the particles (E_m, $\alpha_m < E_p$, α_p).

Crystallographic slip has been observed and the slip system has been identified as [100] {100}, corresponding to prismatic slip. Further, a cross slip phenomenon has been demonstrated.

Acknowledgments

The authors wish to thank Y. Inomata, H. Tanaka and Y. Bando of the National Institute for Research in Inorganic Materials (Tsukuba, Japan) for promoting the use of the JEOL 2000 EX HREM equipment and for their kind cooperation. K. Niihara of the ISIR (Osaka University, Japan), is also acknowledged for fruitful discussions.

References

1. Niihara, K., Ishizaki, K. & Kawakami, T., Hot-pressed Si_3N_4-32% SiC nanocomposite from amorphous Si–C–N powder with improved strength above 1200 C. *J. Mat. Sci. Lett.*, **10** (1990) 112–14.
2. Izaki, K., Hakkei, K., Ando, K., Kawakami, T. & Niihara, K., Fabrication and mechanical properties of Si_3N_4–SiC composites from fine, amorphous Si–C–N powder precursors. In *Ultrastructure processing of advanced ceramics*, ed. J. D. Mackenzie & D. R. Ulrich. John Wiley & Sons, Inc., USA, 1988, pp. 891–900.
3. Niihara, K., Hirano, T., Nakahira, A., Ojima, K. & Izaki, K., High-temperature performance of Si_3N_4–SiC composites from fine, amorphous Si–C–N powder. *MRS Int'l Mtg on Adv. Mat.*, **5** (1989) 107–12.
4. Wakai, F., Kodama, Y., Sakaguchi, S., Murayama, N., Izaki, K. & Niihara, K., A superplastic covalent crystal composite. *Lett. to Nature*, **344** (1990) 421–23.
5. Niihara, K., Suganuma, K., Nakahira, A. & Izaki, K., Interfaces in Si_3N_4–SiC nanocomposite. *J. Mat. Sci. Lett.*, **9** (1990) 598–599.

6. Sasaki, G., Nakase, H., Suganuma, K., Fujita, T. & Niihara, K., Observation of fracture path of SiC particle dispersed Si_3N_4 composites. *Proc. 1st Inter. Symp. on the Sci. of Engineering Cer.*, (1991), pp. 291–6.
7. Butler, E., Observations of dislocations in β-silicon nitride. *The Phil. Mag., 8th series*, **24** (1971) 829–34.
8. Kakibayashi, H., Shimotsu, T. & Nagata, F., Fine structure of crack in yttrium oxide and aluminium oxide fluxed silicon nitride. *J. Electron Microsc.*, [34] 2 (1985) 78–84.
9. Sasaki, K., Kuroda, K., Imura, T., Saka, H. & Kamino, T., Determination of the displacement vector of planar defects in α silicon nitride whiskers by means of high resolution electron microscopy. *J. Electron Microsc.*, [34] 4 (1985) 414–18.
10. Olsson, P. O., Crystal defects and coherent intergrowth of α- and β-crystals in Y-Ce doped sialon materials. *J. Mat. Sci.*, **24** (1989) 3878–87.
11. Rouxel, T., Wakai, F. & Izaki, K., Tensile ductility of superplastic Al_2O_3–Y_2O_3–Si_3N_4/SiC composites. *J. Am. Ceram. Soc.*, **75** (1992) 2363–72.
12. Chin, G. Y., Slip and twinning systems in ceramic crystals. In *Fracture Mechanics of Ceramics*, Vol. 1, ed. R. C. Bradt, D. P. H. Hasselman & F. F. Lange. Plenum Press, New York (1975), pp. 25–59.
13. Bacon, D. J. & Martin, J. W., The atomic structure of dislocations in hcp metals: 1-Potentials and unstressed crystals. *Phil. Mag. A*, [43] 4 (1981) 883–900.
14. French, D. N. & Thomas, D. A., Hardness anisotropy and slip in WC crystals. *Trans. of the Metallurgical Soc. of AIME*, **233** (1965) 950–2.
15. Faber, K. T. & Evans, A. G., Crack deflection processes—1. Theory. *Acta. Metall.*, [31] 4 (1983) 565–76.
16. Krstic, V. D. & Khaund, A. K., Conditions for toughening of particulate brittle composites. In *Advances in Fracture Research* (Fracture 81), ed. D. Francois (Pergamon press), 4 (1981) 1577–85.
17. Selsing, J., Internal stresses in ceramics. *J. Am. Ceram. Soc.*, Discussions and Notes, August (1961) 419.
18. Engineering Materials Handbook, Vol. 4, Ceramics and glasses. ASM International, page 191 (1991).
19. Sakaguchi, S., Murayama, N., Kodama, Y. & Wakai, F., The Poisson's ratio of engineering ceramics at elevated temperature. *J. Mat. Sci. Lett.*, **10** (1991) 282–4.